First-principles determination of static potential energy surfaces for atomic friction in MoS$_2$ and MoO$_3$

Tao Liang,[1] W. Gregory Sawyer,[1,2] Scott S. Perry,[1] Susan B. Sinnott,[1] and Simon R. Phillpot[1,*]

[1]*Department of Materials Science and Engineering, University of Florida, Gainesville, Florida 32611, USA*
[2]*Department of Mechanical and Aerospace Engineering, University of Florida, Gainesville, Florida 32611, USA*

Using first-principles electronic-structure calculations of static potential energy surfaces, we investigate the atomic-scale energetic barriers encountered during sliding at MoS$_2$ (001) and MoO$_3$ (001) surfaces and at the MoS$_2$/MoO$_3$ interface. The results indicate the minimum energy path to sliding and provide an upper bound to the force that must be applied in order to initiate sliding. The results further suggest that the lowest energy pathway is to slide MoO$_3$ over MoS$_2$ along the channel direction formed by S atoms at the sliding interface, and the highest energy pathway involves MoO$_3$ (001) interlayer sliding, which is consistent with the results of experimental microscopic investigations of similar crystalline interfaces.

I. INTRODUCTION

Results from sophisticated new experimental tools for friction studies, such as atomic force microscopy (AFM), are greatly increasing our mechanistic understanding of tribology.[1] Continuing increases in computational power are also allowing complementary simulation approaches to provide powerful insights. Owing to the atomic or molecular nature of nanoscale friction, sophisticated descriptions of atomic bonding and electron density can now be used to calculate the interactions between sliding surfaces. Friction force calculations have been performed either analytically,[2] by first-principles calculations,[3–5] or using empirical potentials in molecular dynamics simulations.[1,6] Quantum mechanics based first-principles methods are widely recognized as a powerful tool to examine the nature and consequences of the interactions between surfaces at the nanometer scale.

As a widely used solid lubricant, MoS$_2$ has been intensively studied both theoretically[3,5] and experimentally.[7–9] While a number of hypotheses have been proposed to explain the experimentally observed exceptional frictional properties of MoS$_2$ in vacuum, and its deterioration when it is exposed to air, no clear consensus has yet emerged. Simulation has the potential of providing significant insights into the tribological properties of MoS$_2$ and MoO$_3$.

Previously, the static potential energy surface of MoO$_3$/MoS$_2$ was calculated by Smith *et al.*[5] using tight-binding simulation methods. Their results qualitatively explained the friction anisotropy of the MoO$_3$/MoS$_2$ system seen in AFM studies by Sheehan and Lieber.[7] Here, we characterize the energetics of barriers to sliding MoS$_2$ and MoO$_3$ surfaces and of sliding at MoO$_3$/MoS$_2$ interfaces using density-functional theory (DFT) calculations.

II. MODELS AND COMPUTATIONAL DETAILS

MoS$_2$ has a lamellar crystal structure formed by stacking S-Mo-S trilayers.[3,10,11] The central layer of Mo atoms forms an equilateral triangle; this layer is sandwiched between two other equilateral triangular layers of S atoms (Fig. 1). Each Mo atom lies at the center of the triangular prism formed by its six neighboring S atoms to form a MoS$_6$ unit. The bonding in the MoS$_6$ unit is mainly covalent in nature and thus strong. By contrast, the S-Mo-S trilayers are weakly bonded to each other by the van der Waals (vdW) forces. The MoS$_2$ conventional unit cell is hexagonal with lattice parameters of $a=0.316$ nm and $c=1.229$ nm. It is convenient to construct an orthorhombic unit cell, in which the orthorhombic [100], [010], and [001] directions correspond to the hexagonal [1$\bar{1}$00], [11$\bar{2}$0], and [0001] directions, respectively. The lattice parameters of this orthorhombic unit cell, which contains four MoS$_2$ f.u., are $a=0.547$ nm, $b=0.316$ nm, and $c=1.229$ nm. The static potential energy surface calculations of the MoS$_2$ (001) surface are performed on a $2 \times 2 \times 2$ orthorhombic unit cell (i.e., M$_{32}$S$_{64}$). A vacuum region of 1 nm thickness is added in the [001] direction, such that the nonsliding surfaces do not interact.

MoO$_3$ forms an orthorhombic layered crystal structure. Each layer comprises two interleaved planes of MoO$_6$ octahedra, as illustrated in Fig. 2. The oxygen atoms in the MoO$_6$ unit are labeled O1, O2, and O3 in Fig. 2, respectively, since each of them has one, two, or three Mo neighbors. Detailed structural information for MoO$_3$ is available,[12–14] which indicates that the interactions between Mo and O atoms are dominated by strong ionic and covalent bonding, while the
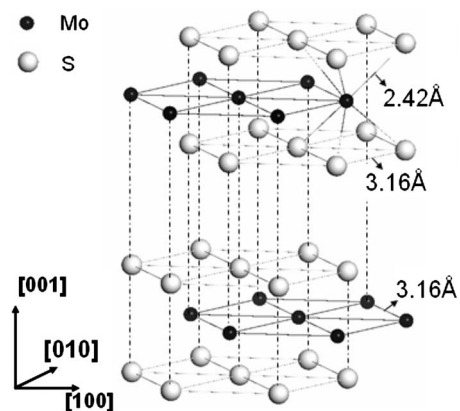
FIG. 1. Crystal structure of MoS$_2$.

(a)

Top view of sliding interface

(b)
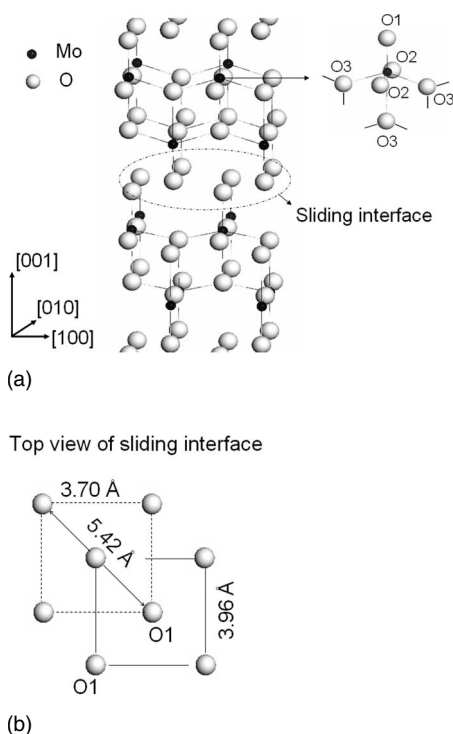
FIG. 2. Crystal structure of MoO_3.

FIG. 3. Atomic configuration of MoO_3/MoS_2 interface.

individual layers parallel to the (001) plane are coupled by the weak van der Waals forces, as in MoS_2. Because the ideal (001) plane with the O1 atom exposed on the surface represents the lowest energy cleavage plane, the static potential energy surface calculations consider the sliding of one MoO_3 (001) surface on another. A top view of the MoO_3 sliding interface is given in Fig. 2. The lattice parameters for the conventional orthorhombic cells of four MoO_3 f.u. are a =0.370 nm, b=0.396 nm, and c=1.385 nm. The MoO_3 simulation supercell consists of $2 \times 2 \times 2$ MoO_3 orthorhombic unit cell of 128 atoms ($Mo_{32}O_{96}$). As with MoS_2, a vacuum region of 1 nm thickness in the [001] direction ensures that the outer surfaces do not interact.

In constructing a MoS_2/MoO_3 layered system, a choice has to be made as to the relative orientations of each material; the criterion we use is to minimize any in-plane strain. As shown in Fig. 2, the diagonal distance between the O1 atoms on the (001) surface of MoO_3 is 0.542 nm, which is very close to the [010] length of the MoS_2 unit cell (0.547 nm). A nearly strain-free MoO_3/MoS_2 interfacial structure is constructed by rotating and then attaching a 3 $\times 4 \times 1$ MoO_3 slab on top of a $2 \times 5 \times 1$ orthorhombic MoS_2 such that the MoO_3 (001) surface is parallel to the MoS_2 (001) surface and the MoO_3 [110] direction is parallel to the MoS_2 [010] direction; the resulting lattice mismatches are 1.8% in the [001] direction and 0.2% in the [010] direction. A schematic of the MoO_3/MoS_2 interface is given in Fig. 3. This MoO_3/MoS_2 model contains 20 MoS_2 f.u. and 24 MoO_3 f.u. for a total of 156 atoms. It would, of course, be desirable to reduce the in-plane strain even further. However, the next commensurate system size would need to be 1310 ($Mo_{370}O_{600}S_{340}$) atoms, which is beyond our current capabilities. Here also, there is a 1 nm vacuum in the [001] direction of the MoO_3/MoS_2 model.
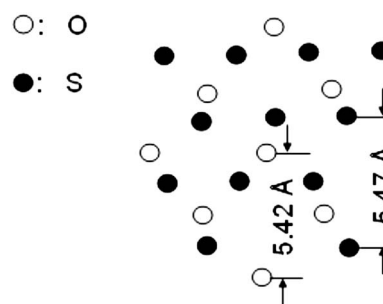
The rapid increase in computer capabilities has allowed this effort to make two significant technical advances over the approach used by Smith *et al.*:[5] the model used here is about three times larger and the interatomic interactions are described by DFT, which should give better material fidelity than the less-sophisticated tight-binding method.

All of the calculations are performed with the plane-wave density-functional theory software code VASP (Vienna *ab initio* simulation package) using the local density approximation (LDA) pseudopotentials with the core electron correction for Mo. The cutoff energy is 270 eV, which yields a total energy that is approximately the same as higher, more computationally intensive cutoff energies of 400 and 600 eV. In addition, each calculation has an energy convergence of no more than 0.001 eV per surface atom. With these settings, the calculated lattice parameters for bulk hexagonal MoS_2 are a=0.312 nm (experimental value of 0.316 nm) and c =1.211 nm (1.230 nm); for bulk MoO_3, they are a =0.368 nm (0.370 nm), b=0.381 nm (0.396 nm), and c =1.392 nm (1.385 nm). The good agreement of the calculated values with experimental data indicates that the methodologies and program settings used here are effective for reproducing the crystal structures of the systems.

The three input models, with the vacuum present, are first relaxed, without any system shape and volume change allowed. Each system is then placed under an external load by manually compressing the system in the Z direction [normal to the sliding surface, as indicated in Fig. 4(a)] and then pinning the atoms (S or O) on the top atomic plane of the upper trilayer and on the bottom plane of the lower layers. The compressed system is thereafter equilibrated until the measured force on the atoms on the top and bottom planes differs by no more than 0.01 nN, indicating that the stress is uniform through the system. By repeatedly compressing the system and then measuring the forces of the resulting system, the target pressure is reached in a rapid and accurate manner. The target pressure for all the three systems is 500 MPa, which corresponds to a force of 0.33 nN (0.041 nN per S atom) for MoS_2. The normal load vs strain (%) for the contact of two trilayers of MoS_2 is plotted in Fig. 4(b).

After the 500 MPa target pressure is reached, the static potential energy surface is mapped at different positions by rigidly moving the top half of the compressed system in the X and Y directions (parallel to the sliding interface), as indicated in Fig. 5. The forces on the resulting system are then fully relaxed, and the system energy is compared with the

(a)

(b)
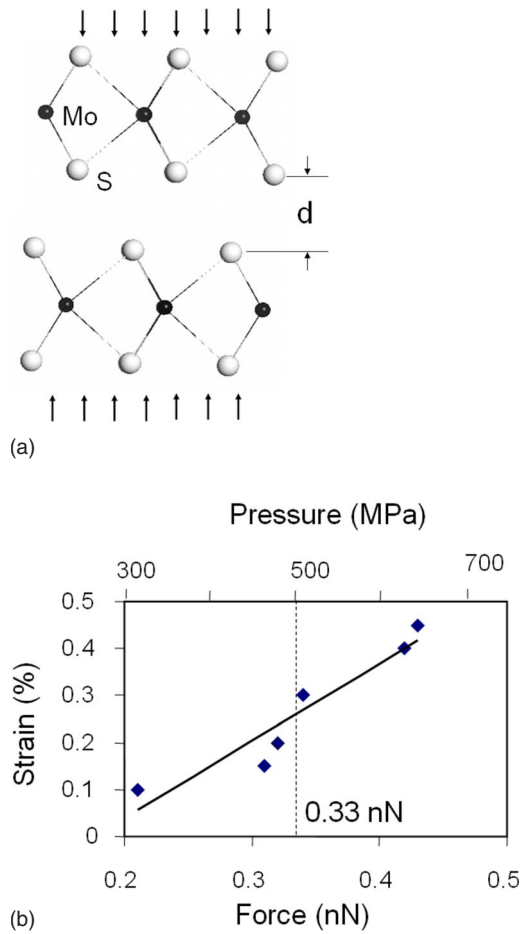
FIG. 4. (Color online) Compressing the system. (a) A schematic view of compressing MoS_2 system. (b) Normal load or force vs strain $(d_0-d)/d_0$, where $d_0=0.29$ nm. d_0 is the separation between MoS_2 trilayers at equilibrium and d is the separation under pressure.

energy of the initial untranslated compressed system.

It is worthwhile to note that there is a concern of using conventional DFT-LDA to describe the vdW interactions in the layered structures.[15–17] However, it is well documented that the overbinding in the conventional LDA can result in a cancellation of errors,[15] which yields reasonable modeling of the vdW interactions. Importantly, the systems under consideration here are all subjected to compressive forces. Thus, the dominant force between the weakly bonded layers is electron repulsion which is well described by conventional LDA pseudopotentials.[15] Last, the data reported here are
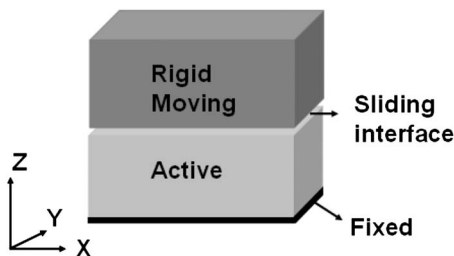
FIG. 5. A schematic illustration of the initial setups of the models for potential energy surface calculations.
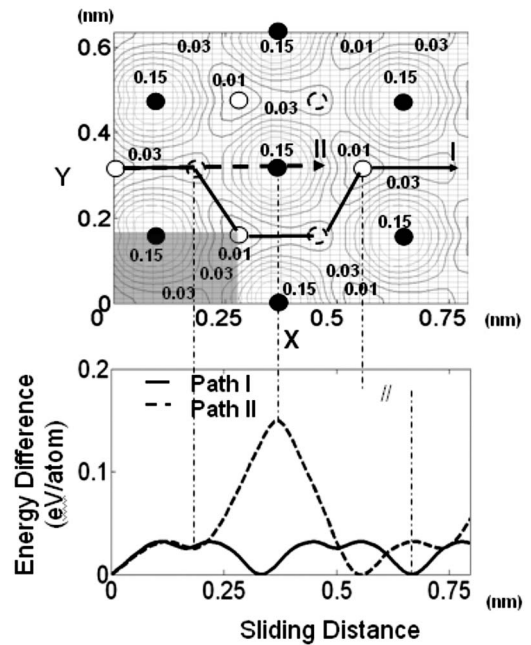
FIG. 6. Static potential energy surface of MoS_2 as a function of positions. Top: contour plot of energy difference as a function of displacement in X and Y directions (parallel to the sliding surface). Open circles represent S atoms on the top of sliding interface and solid circles represent S atoms underneath. Calculations are only performed within the shaded area; the rest of the figure is generated based on the surface symmetry and is included for clarity. Bottom: energy difference along the sliding pathways.

relative values between translated and untranslated systems. As indicated in Ref. 16, the qualitative and quantitative energy differences determined in the compressive regime of vdW interactions using the conventional LDA are suitable for the work discussed here.

III. RESULTS AND DISCUSSION

The static potential energy surfaces for interlayer sliding of the MoS_2 (001)/MoS_2 (001), MoO_3 (001)/MoO_3 (001), and MoO_3 (001)/MoS_2 (001) interfaces are shown in Figs. 6–8, respectively. The contour plot at the top of each figure maps the potential energy surface as a function of displacement in the X and Y directions, as determined from the DFT calculations. The dark shaded area represents the periodically repeating planar unit cell of the surface. Within this area, the energy was determined on a 6×5 grid in the X-Y plane. The potential-energy surface determined at these 6×5 individual points is repeated a number of times in X and Y to enable the energy surface to be more clearly seen as the lightly shaded area. The open circles represent the positions of atoms at the sliding interface from the top slab, in specific, S for MoS_2, O for MoO_3, and O for MoO_3/MoS_2. The solid circles represent atoms at the top atomic plane of the lower sliding surface, which are S for MoS_2, O for MoO_3, and S for MoO_3/MoS_2.

As shown in Fig. 1, the S atoms on the (001) surface of MoS_2 form an array of equilateral triangles. There are two
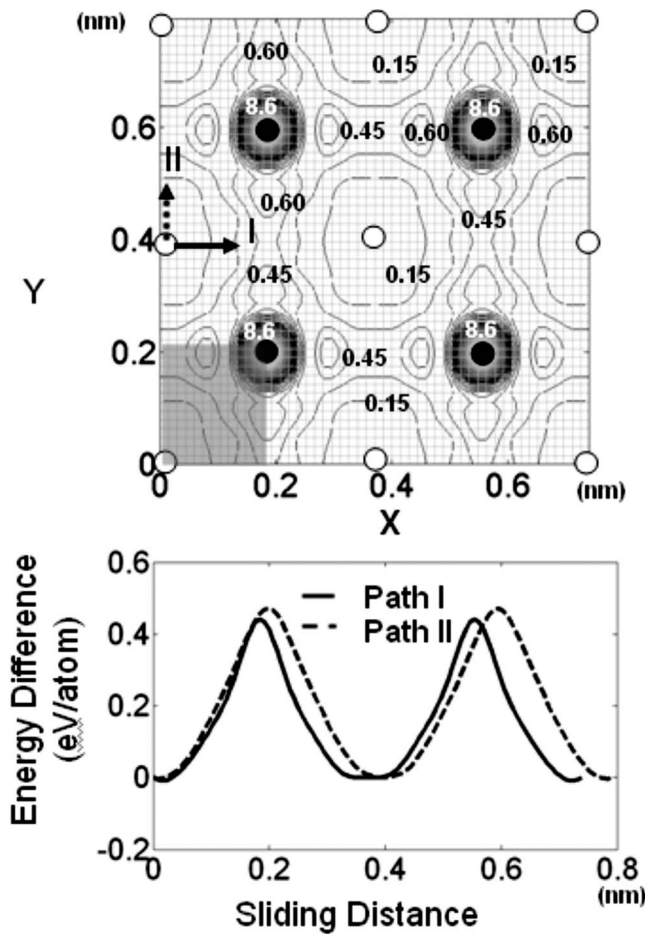
FIG. 7. Static potential energy surface of MoO_3 as a function of position. Top: contour plot of energy difference as a function of displacement in X and Y directions (parallel to the sliding surface). Open circles represent O atoms on the top of sliding interface and solid circles represent O atoms underneath. Bottom: energy difference along the sliding pathways.

equivalent arrangements of this two-dimensional (2D) net. One is shown by the solid circles in Fig. 6, and it indicates the positions of the S atoms at the sliding interface from the top slab. The other equivalent arrangement is shown by the dashed open circles. As indicated in Fig. 6, the maximum energy of 0.15 eV/atom occurs when the S atoms at the sliding interfaces are right on top of each other. However, the energy at the dashed open circles is only 0.03 eV/atom.

From this energy surface, it is possible to predict the energetically favored path taken during sliding. In order to avoid the peak energy barrier, the upper MoS_2 layer will take a "zigzag" route (path I) over the positions indicated by the dashed open circles. The more direct route (path II) is strongly unfavorable because of the large energy peaks. Such zigzag paths are also predicted in potential surfaces similar to the MoS_2 (001) surface, such as the graphite or diamond (111) surface.[1,2]

As shown in Figs. 2 and 7, the O layers of MoO_3 (001) sliding interface form two rectangular 2D lattices translated to each other by [1/2, 1/2]. In the perpendicular direction (Z direction), the spacings between oxygen planes in neigh-
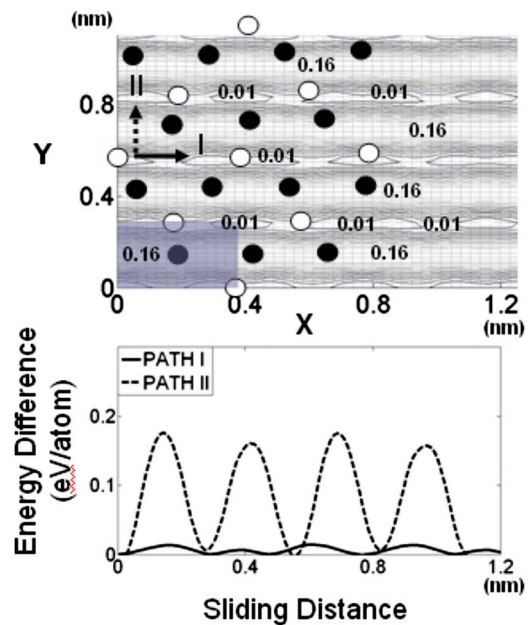
FIG. 8. (Color online) Static potential energy surface of MoO_3/MoS_2 as a function of positions. Top: a contour plot of energy difference as a function of displacement in X and Y directions (parallel to the sliding surface). Open circles represent O atoms on the top of sliding interface and solid circles represent S atoms underneath. Bottom: energy difference along the sliding pathways.

boring trilayers are 0.071 nm at zero pressure and 0.066 nm under a pressure of 500 MPa. These remarkably small spacings between the sliding surfaces result from the commensurability of the opposing surfaces of low electronic corrugation and lead to a prohibitively high energy of 8.6 eV/atom when the O atoms are on the top of each; this configuration is reached by diagonal motion of the top layer over the bottom layer. Comparing the two paths indicated in Fig. 7, sliding along path I along the [100] direction has an energy peak of 0.44 eV/atom, which is about 0.03 eV/atom lower than the energy peak along path II, which along the [010] direction. This is due to the difference of lattice parameters in the [100] and [010] directions (0.370 vs 0.396 nm), with the slightly larger spacing between the two (100) planes allowing the O atoms to more easily slide along the [100] direction.

In the MoO_3/MoS_2 model, the O atoms of the MoO_3 slab are located in the channels formed by the S atoms of MoS_2 substrate (Fig. 8). For motion perpendicular to the S channel direction, [010], the energy maximum is 0.18 eV/S atom. By contrast, along the S channels, [100], the energy maximum is only 0.013 eV/S atom. The potential surface has essentially the same shape as predicted by the tight-binding calculations of Smith *et al.*[5] However, they predicted an energy maximum of 0.04 eV/S atom for sliding perpendicular to the channel direction at zero pressure. Limited by computer resources available at the time their study was carried out, their MoO_3/MoS_2 model consisted of 56 atoms ($Mo_{16}O_{24}S_{16}$) and was heavily distorted. With a larger system, and a more precise description of the interactions in the system, the value predicted by our calculation should be more accurate. Con-

TABLE I. Estimated friction force along the preferred path (path I in each of Figs. 6–8).

Systems	Normal force (nN/atom)	Lateral friction force (nN/atom)
MoS_2	0.042	0.058
MoO_3	0.086	0.352
MoO_3/MoS_2	0.070	0.011

sistent with the model proposed by Sheehan and Lieber[7] and by Smith *et al.*,[5] these results demonstrate that friction anisotropy can be predicted from static potential energy surface calculations of the MoO_3/MoS_2 model.

Using the potential energy surfaces in Figs. 6–8, we can estimate the lowest energy paths for interlayer sliding. Moreover, the critical friction force that needs to be applied to move the upper slab can be estimated.[4,5] To illustrate the approach, consider a simple system of two rigid commensurate lattices separated by an atomically flat interface at zero temperature. Suppose that the system starts from an energy minimum and an external lateral force normal (i.e., parallel to the interface) is applied to slide one surface over the other. Assume the lateral force is just large enough to move the upper slab and slowly approach to the energy maximum. The energy difference between the energy maximum and energy minimum is the work that must be done to the system by the external lateral force. Therefore, the critical (i.e., minimum) lateral force that has to be applied to move the system then can be estimated as the slope of the different energy paths in Figs. 6–8. The critical lateral forces for the three systems are shown in Table I. Based on these values, the MoO_3/MoS_2 has the lowest critical sliding force, with sliding taking place along the S channel direction, while MoO_3 (001) should have the highest regardless of orientation.

The above analysis is, of course, a significant oversimplification of the experimental situation in which layers do not likely move as rigid blocks. Instead, in a physical system, it is likely that some regions will slip, while others do not. The regions that do slip will not settle fully into their local minima and will interact elastically with other regions that have not slipped. Thus, the predicted critical sliding forces based on this approach can be expected to generally be larger than the experimental values. In previous theoretical investigations of the tribological response of graphite, Zhong and Tomanek determined the ratio of the calculated critical friction force and applied load as a measure of the friction coefficient. This interpretation seems to be potentially problematic because the energy surfaces are intrinsically measures of the reversible work required to slide the layers over each other, rather than the dissipative energy loss associated with friction. As such, only energetic barriers to sliding are reported here.

These limitations notwithstanding, the results in Table I portray a trend in the sliding behavior as a function of com-

position, in close agreement with previous experimental measurements. The shear stress (friction force divided by contact area) σ of MoS_2 determined from macroscopic experiments in a dry air environment is about 24.8 MPa. In contrast, AFM friction data at sliding MoO_3/MoS_2 interfaces yield $\sigma = 1.1$ MPa.[7] Although these measurements have been conducted on different length scales, they clearly portray a greater resistance to sliding for the self-mated interface, in agreement with the results of our calculation. Unfortunately, no experimental values of shear stress (or friction coefficient) for interlayer sliding between pristine MoO_3 (001) surfaces have reported. However, Klein and Mathey[18] performed a set of AFM experiments and measured the friction force of moving a Si (111) tip across the MoS_2 (001) and α-MoO_3 (001) surfaces. They suggested that MoO_3 has a larger friction coefficient than MoS_2 due to the larger interlayer cohesion (proportional to shear stress) in MoO_3. In a comparison of MoS_2 and oxidized MoS_2 coatings performed on macroscopic pin-on-disk experiments, Fleischauer and Lince[9] stated that MoO_3 can display reasonably low friction coefficients but not nearly as low as that of MoS_2. In a general sense, our calculations predict the same trend in MoS_2 and MoO_3 interlayer slidings.

IV. CONCLUSIONS

Using first-principles electronic-structure methods, we have calculated the static potential energy surface of MoS_2 (001) and MoO_3 (001) surfaces and of the MoO_3 (001)/MoS_2 (001) interface under pressures of 500 MPa applied normal to the sliding interface. The atomic configuration at the sliding interface is a key factor to determine the topology of the potential energy surface. From the potential energy surface, we have directly obtained the energetic barriers to sliding associated with various sliding pathways. The relative values suggest that it is easiest to move MoO_3 over MoS_2 along the channel direction formed by S atoms at the sliding surface and hardest for MoO_3 (001) interlayer sliding, which is in general agreement with experimental observations. The oxidation of MoS_2 to form MoO_3 generally has an adverse effect on lubrication properties. However, both calculations and experiments suggest that friction between pristine MoO_3/MoS_2 interfaces is extremely small along the channel direction, even smaller than that of MoS_2. Greater insight into the adverse effects associated with oxidation awaits larger calculations considering surface defects and the formation of noncrystalline surfaces, as well as atomic-scale experimental interrogation of such interfaces.

*Corresponding author. sphil@mse.ufl.edu

[1] I. L. Singer, J. Vac. Sci. Technol. A **12**, 2605 (1994).

[2] H. M. Katsuyoshi Matsushita, and Naruo Sasaki, Solid State Commun. **136**, 51 (2005).

[3] F. R. H. Chermette, O. El Beqqali, J. F. Paul, C. Donnet, J. M. Martin, and T. Le Mogne, Surf. Sci. **472**, 97 (2001).

[4] W. Zhong and D. Tomanek, Phys. Rev. Lett. **64**, 3054 (1990).

[5] G. S. Smith, N. A. Modine, U. V. Waghmare, and E. Kaxiras, J. Comput.-Aided Mater. Des. **5**, 61 (1998).

[6] J. D. Schall and D. W. Brenner, Mol. Simul. **25**, 73 (2000).

[7] P. E. Sheehan and C. M. Lieber, Science **272**, 1158 (1996).

[8] J. M. Martin, C. Donnet, Th. Le Mogne, and Th. Epicier, Phys. Rev. B **48**, 10583 (1993).

[9] P. D. Fleischauer and J. R. Lince, Tribol. Int. **32**, 627 (1999).

[10] I. Z. O. El Beqqali, F. Rogemond, H. Chermette, R. Ben Chaabane, M. Gamoudi, and G. Guillaud, Synth. Met. **90**, 165 (1997).

[11] R. P. Valentin Alexiev, Phys. Chem. Chem. Phys. **2**, 1815 (2000).

[12] X. L. Yin, H. M. Han, and A. Miyamoto, J. Mol. Model. **7**, 207 (2001).

[13] K. Hermann, M. Witko, and A. Michalak, Catal. Today **50**, 567 (1999).

[14] M. Chen, U. V. Waghmare, C. M. Friend, and E. Kaxiras, J. Chem. Phys. **109**, 6854 (1998).

[15] L. A. Girifalco and M. Hodak, Phys. Rev. B **65**, 125404 (2002).

[16] H. Rydberg, B. I. Lundqvist, D. C. Langreth, and M. Dion, Phys. Rev. B **62**, 6997 (2000).

[17] H. Rydberg, M. Dion, N. Jacobson, E. Schröder, P. Hyldgaard, S. I. Simak, D. C. Langreth, and B. I. Lundqvist, Phys. Rev. Lett. **91**, 126402 (2003).

[18] D. P. H. Klein and Y. Mathey, Surf. Sci. **387**, 227 (1997).